Bioactive Materials 51 (2025) 318–332

Contents lists available at ScienceDirect

Bioactive Materials

journal homepage: www.keaipublishing.com/en/journals/bioactive-materials

An "inside-out"-guided genetically engineered hydrogel for augmenting aged bone regeneration

Yanrun Zhu [a,b,f,1], Lili Sun [c,d,1], Mingzhuang Hou [a,b,1], Jianfeng Yu [a,b], Chenqi Yu [a,b], Zihan Zhang [g], Huilin Yang [a,b], Changsheng Liu [c,d], Lixin Huang [a,b], Dinghua Jiang [a,b,*], Yijian Zhang [a,b,**], Yuan Yuan [c,d,***], Xuesong Zhu [a,b,e,****]

[a] Department of Orthopaedics, The First Affiliated Hospital of Soochow University, Soochow University, Suzhou, 215006, China
[b] Orthopaedic Institute, Medical College, Soochow University, Suzhou, 215000, China
[c] Key Laboratory for Ultrafine Materials of Ministry of Education, School of Materials Science and Engineering, East China University of Science and Technology, Shanghai, 200237, China
[d] Engineering Research Center for Biomedical Materials of Ministry of Education, East China University of Science and Technology, Shanghai, 200237, China
[e] Department of Orthopaedics, The Affiliated Suzhou Hospital of Nanjing Medical University, Suzhou Municipal Hospital, Gusu School, Nanjing Medical University, Suzhou, 215002, China
[f] Xuzhou Medical University Affiliated Hospital Sihong Branch, The First People's Hospital of Sihong County, Suqian, 223900, China
[g] Xi'an Jiaotong-Liverpool University, Suzhou, 215123, China

ARTICLE INFO

Keywords:
Senile bone regeneration
Senescent bone marrow-derived stem cells
Senescent associated secretory phenotype
Sirtuins 3
Hypoxia hydrogels

ABSTRACT

Senescent bone repair faces significant obstacles due to reduced cellular activity and an unfavorable microenvironment, both of which hinder the osteogenic differentiation of bone marrow-derived stem cells (BMSCs) into osteoblasts (OBs) and subsequent bone formation. Current approaches primarily target senescent cell clearance (senolytics) or suppression of the senescence-associated secretory phenotype (senomorphics), neglecting the complex interactions between BMSCs and the osteogenic microenvironment. In this study, a genetically engineered hydrogel incorporating NAD-dependent deacetylase sirtuins 3 (SIRT3)-loaded nano-vectors and poly (glycerol sebacate)-co-poly (ethylene glycol)/polyacrylic acid (PEGS/PAA) was developed as an "inside-out" strategy for bone regeneration. At the intracellular level, BMSC function is restored, and osteogenesis is promoted through genetically enhanced SIRT3 expression. At the extracellular level, carboxyl functional groups chelate iron ions, simulating a hypoxic environment and promoting synergistic interactions between angiogenesis and osteogenesis. The therapeutic effects of the genetically engineered hydrogel in alleviating senescent damage and enhancing osteogenic differentiation were confirmed in both chemically and naturally induced senescence models *in vitro*. Local delivery of the hydrogel significantly increased newly formed bone in rat cranial defects. Mechanistically, the central role of SIRT3 in balancing senescence and osteogenesis, as well as its involvement in bone immune signaling pathways, was elucidated through CRISPR/Cas9-mediated editing in mice and transcriptome sequencing. This work presents a novel paradigm that integrates cellular and microenvironmental factors to enhance bone regeneration, offering new hope for treating age-related bone injuries.

Peer review under the responsibility of editorial board of Bioactive Materials.

* Corresponding author. Department of Orthopaedics, The First Affiliated Hospital of Soochow University, Soochow University, Suzhou, 215006, China.
** Corresponding author. Department of Orthopaedics, The First Affiliated Hospital of Soochow University, Soochow University, Suzhou, 215006, China.
*** Corresponding author. Key Laboratory for Ultrafine Materials of Ministry of Education, School of Materials Science and Engineering, East China University of Science and Technology, Shanghai, 200237, China.
**** Corresponding author. Department of Orthopaedics, The First Affiliated Hospital of Soochow University, Soochow University, Suzhou, 215006, China.
E-mail addresses: jdhyzjyh@126.com (D. Jiang), zhangyijian@suda.edu.cn (Y. Zhang), yyuan@ecust.edu.cn (Y. Yuan), zhuxs@suda.edu.cn (X. Zhu).
[1] These authors contributed equally to this work.

https://doi.org/10.1016/j.bioactmat.2025.05.003
Received 12 March 2025; Received in revised form 24 April 2025; Accepted 5 May 2025

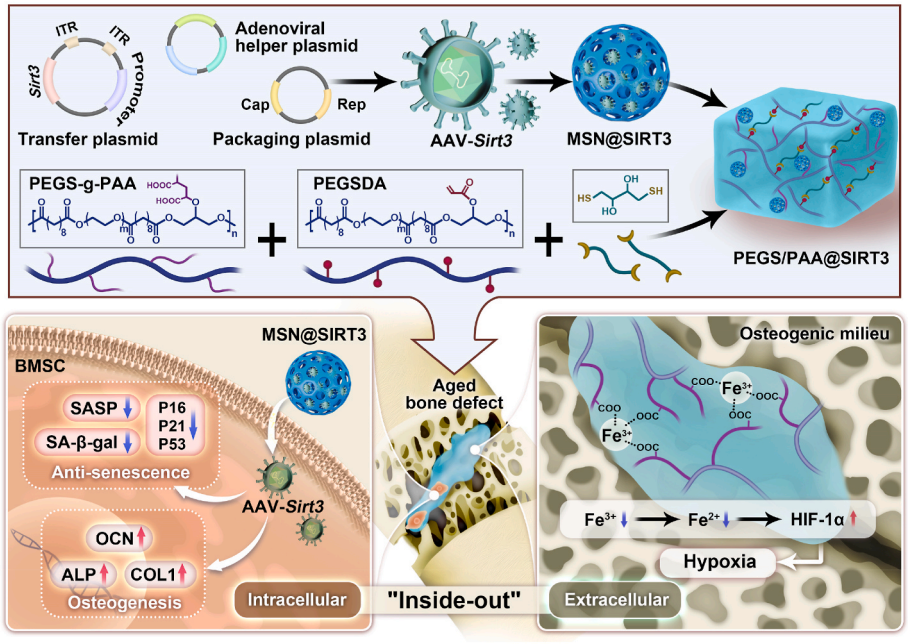

Scheme 1. Design and application of the "inside-out"-guided genetically engineered hydrogel for aged bone injury treatment. A genetically engineered hydrogel, incorporating NAD-dependent deacetylase sirtuin 3 (SIRT3)-loaded nano-vectors and poly (glycerol sebacate)-co-poly (ethylene glycol)/poly (acrylic acid) (PEGS/PAA), was developed as an "inside-out" approach for promoting aged bone regeneration. At the cellular level, SIRT3 overexpression enhances osteogenic differentiation and mitigates age-associated damage in BMSCs (internal cues). At the extracellular level, carboxyl groups within PEGS/PAA chelate iron ions to mimic HIF-1α-induced hypoxic conditions (external effects). These combined mechanisms delay cellular senescence and facilitate bone healing.

1. Introduction

The remarkable regenerative potential of bone following injury is attributed to the mobilization of endogenous skeletal progenitors, such as bone marrow-derived stem cells (BMSCs) [1], which differentiate into osteoblasts (OBs) and coordinate osteogenesis [2]. In aged native bone, however, the osteogenic differentiation capacity of BMSCs is significantly impaired, resulting in reduced bone formation and delayed or failed healing [3]. The clearance of senescent cells (SCs) through the synergistic combination of dasatinib and quercetin (D + Q) has been shown to be an effective "senolytic therapy" for combating aging, inducing apoptosis and depletion of SCs [4]. Systematic administration of D + Q not only alleviates the progression of postmenopausal osteoporosis but also accelerates bone formation [5]. Unlike the broader clearance of SCs, the targeted restoration of BMSC function and the reconstruction of the extracellular osteogenic microenvironment, as part of an "external and internal cultivation" approach, hold considerable promise for treating refractory bone injuries [6]. The aging of endogenous stem cells is often marked by a lack of energy, hindering the transition from BMSCs to OBs and impairing bone regeneration [7]. Recent studies have highlighted sirtuins 3 (SIRT3), an NAD-dependent deacetylase, as a key energy regulator that drives aerobic respiratory chains [8]. Overexpression of SIRT3 in BMSCs can reduce inflammasome activity and alleviate periprosthetic osteolysis [9], but its role in promoting bone regeneration in aging conditions and the underlying mechanisms remain unclear.

The concept of "Materiobiology" suggests that intelligently engineered, tissue-adaptable materials can selectively neutralize detrimental biological signals, thereby creating a regenerative environment that supports osteogenesis and accelerates bone repair [10]. Our recent work with sulfated polysaccharides and oligosaccharides, rather than exogenous growth factors, has demonstrated the capacity to engage endogenous macrophages and stimulate the secretion of vascular endothelial growth factor (VEGF), thereby inducing angiogenesis for ischemic disease treatment [11]. Traditional bone repair materials typically rely on the direct differentiation of BMSCs into OBs, facilitating bone formation through intramembranous ossification (IMO) [12]. However, these materials often result in avascular necrosis and degradation of central regions due to insufficient angiogenesis and poor perfusion, leading to osteogenesis failure in aged bone. In contrast, the initial stage of cartilage differentiation during the regenerative phase of endochondral ossification (ECO) requires fewer nutrients and less oxygen. As chondrocytes mature, various cytokines are released, promoting osteogenesis and angiogenesis in the hypertrophic cartilage stage [13]. This approach has garnered significant interest for treating elderly patients [14]. The promotion of ECO requires precise regulation of the hypoxia-inducible factor α (HIF-1α) signaling pathway for optimal outcomes [15]. HIF-1α, a key regulator, induces a hypoxic microenvironment by reducing iron ions, making it essential for bone regeneration [16]. Therefore, the combination of restoring senescent BMSC function and remodeling the extracellular microenvironment can synergistically enhance bone regeneration in challenging aging conditions.

Bone regeneration is a critical area of focus in biomaterials research, with extensive studies on the potential of various polymers for promoting bone healing. Polymers such as polylactic acid (PLA) [17], polylactic-co-glycolic acid copolymer (PLGA) [18], and polycaprolactone (PCL) [19] have been widely investigated for bone regeneration applications. However, modifying these polymers to meet specific needs remains a significant challenge. Poly (glycerol sebacate)-co-poly (ethylene glycol) (PEGS), an elastomer with favorable mechanical properties, excellent biocompatibility, and ease of modification, has emerged as an ideal candidate for bone tissue engineering [20]. During aging, SCs produce reactive oxygen species (ROS), inflammatory cytokines, and the senescence-associated secretory phenotype (SASP), all of which hinder bone regeneration [21]. The specific modification of the side chain of PEGS endows it with versatile functionalities, such as enhanced sensitivity to ROS, which in turn boosts the self-renewal capacity of BMSCs and accelerates bone repair [22]. Inspired by the dual positive effects of hypoxia on both osteogenesis and angiogenesis [23], a PAA-modified PEGS hydrogel (PEGS/PAA) that simulates hypoxic conditions through iron ion chelation was introduced [24]. PEGS/PAA copolymers offer several advantages for bone

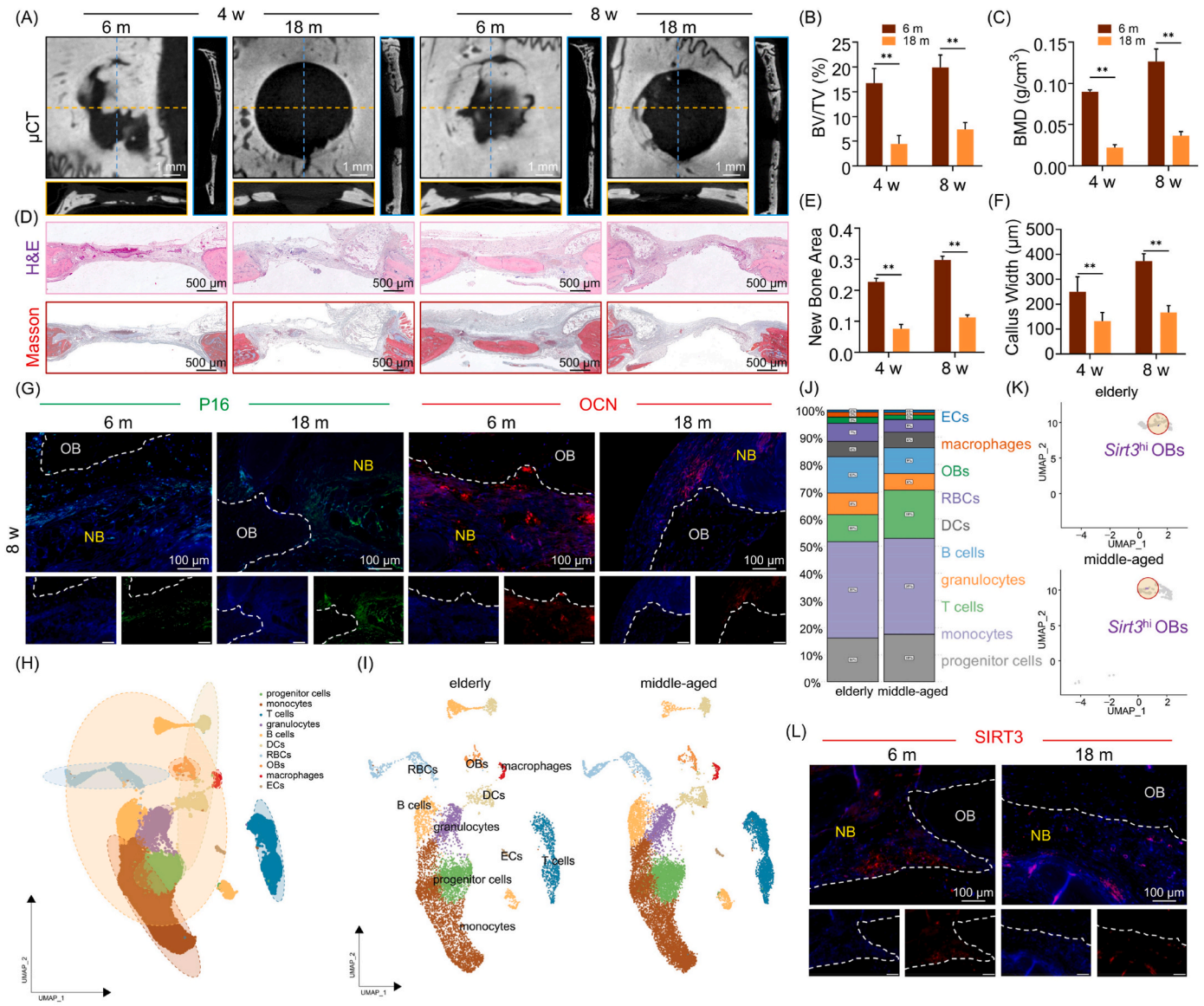

Fig. 1. Evaluation of regenerative capacity in aged bone. (A) New bone formation in the calvarial defect was assessed using micro-CT imaging and 3D reconstruction. Quantitative analysis of the bone volume ratio (BV/TV) (B) and bone mineral density (BMD) (n = 3) (C) in the defect area (n = 3). (D) H & E and Masson's trichrome (MTS) staining images of the defect area. Quantitative analysis of the new bone area (n = 3) (E) and callus width (F) in the defect area (n = 3). (G) Immunofluorescence staining images of P16 and OCN. (H–I) Cellular subpopulations in elderly and middle-aged bone tissue. (J) Proportion of different cell types in elderly and middle-aged bone tissue. (K) Expression of SIRT3-positive osteoblasts in elderly and middle-aged bone tissue. (L) Immunofluorescence staining images of SIRT3 in newborn bone tissue. Data are presented as mean ± standard deviation; $^{*}P < 0.05$, $^{**}P < 0.01$. New bone (NB) and original bone (OB).

regeneration, including their flexibility in incorporating bioactive molecules or pharmaceutical agents. Although PEGS/PAA promotes ECO and contributes to *de novo* bone formation by activating the HIF-1α pathway, further investigation is necessary to fully understand the effects of hypoxia-mimicking hydrogels on aged niches and senile-impaired osteogenesis.

To address the internal energy deficits and the external hostile senescent microenvironment in aged bone repair, this study synthesized the PEGS/PAA@SIRT3 hydrogel, suitable for injection. This hydrogel was created by combining PEGS-g-PAA prepolymers with acrylated PEGS prepolymers, which undergo rapid crosslinking *via* thiol-Michael addition click reaction upon injection. At the cellular level, SIRT3 overexpression rejuvenates the osteogenic capacity and alleviates age-related damage (internal cues), while at the extracellular level, the carboxyl groups within PEGS/PAA chelate iron ions to simulate a hypoxic environment, synergistically enhancing bone repair under aging conditions (external effects). The anti-aging and pro-osteogenic effects, along with their underlying mechanisms, were thoroughly investigated using hydrogen peroxide (H_2O_2)-induced premature senescence and a natural senescence model. The potential applicability and translational efficacy of the PEGS/PAA@SIRT3 hydrogel were comprehensively evaluated in a calvarial defect model in aging rats and *Sirt3*-deficient (*Sirt3*$^{-/-}$) adult mice. This study introduces an innovative gene-hydrogel strategy that restores BMSC function and corrects disturbances in the extracellular microenvironment, demonstrating remarkable "inside-out" efficacy in enhancing bone repair (Scheme 1).

2. Results and discussion

2.1. Impaired bone regeneration in senescence was associated with the decline of SIRT3 expression in BMSCs

Osteogenic differentiation in stem cells plays a critical role in their ability to regenerate bone, whereas the diminished viability of stem cells

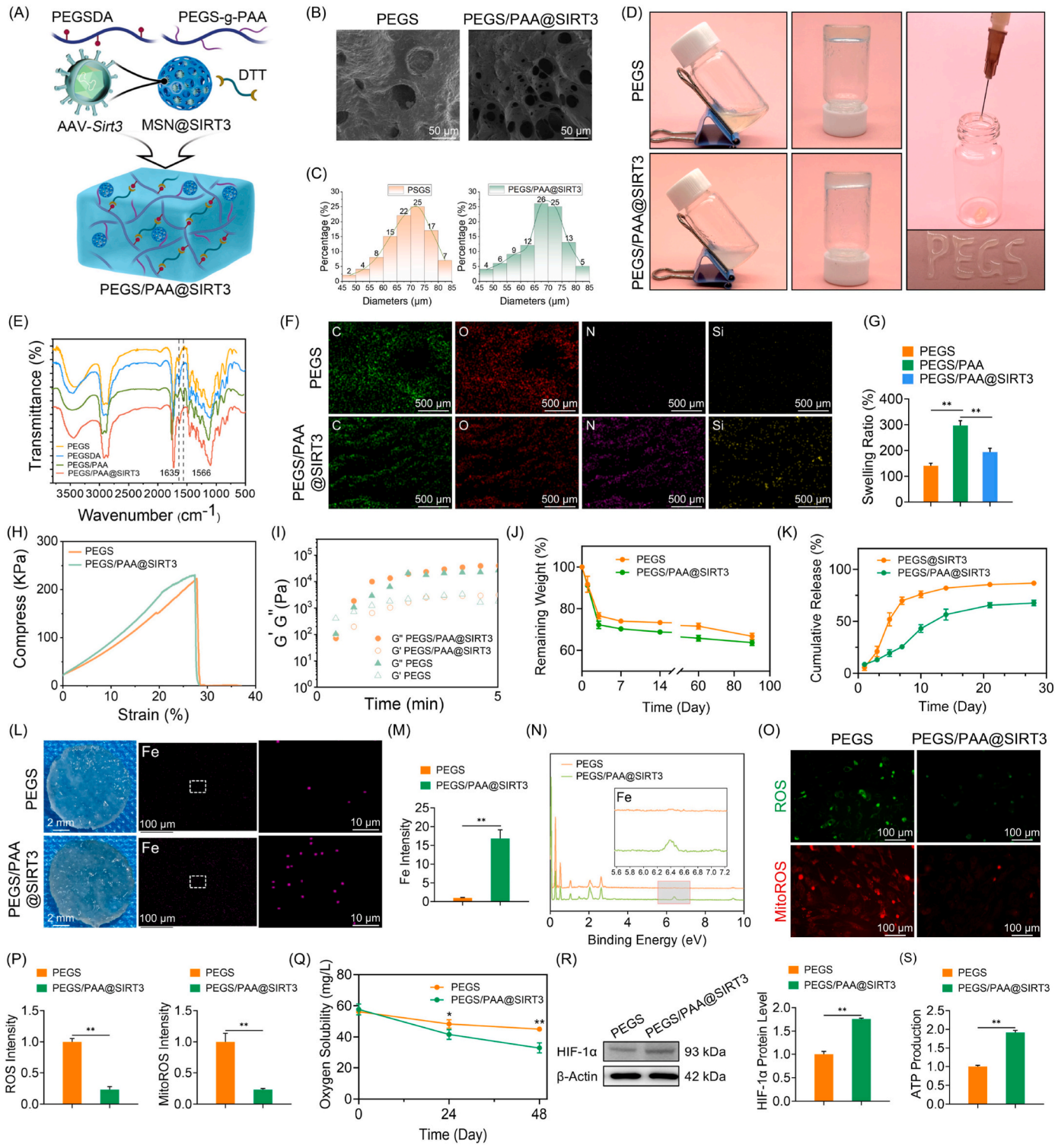

Fig. 2. Fabrication and characterization of PEGS/PAA@SIRT3 hydrogels. (A) Schematic representation of PEGS/PAA@SIRT3 hydrogel fabrication. (B) Ultrastructural parameters visualized by SEM. (C) Quantification of the porosity of PEGS and PEGS/PAA@SIRT3 hydrogels. (D) General view, gelling properties, and injectable properties of the hydrogels. (E) FTIR spectra of PEGS, PEGSDA, PEGS/PAA, and PEGS/PAA@SIRT3 polymers. (F) Energy-dispersive spectroscopy (EDS) elemental mappings. (G) Swelling rate of PEGS and PEGS/PAA@SIRT3 hydrogels (n = 3). (H) Representative stress relaxation curves of PEGS and PEGS/PAA hydrogels. (I) Rheological properties of PEGS and PEGS/PAA@SIRT3 hydrogels. (J) Degradation behaviors of PEGS and PEGS/PAA@SIRT3 hydrogels (n = 3). (K) Cumulative release of SIRT3 from PEGS and PEGS/PAA@SIRT3 hydrogels (n = 3). (L–M) Iron ion chelating ability of PEGS and PEGS/PAA@SIRT3 hydrogels. (N) EDS spectrum of elemental composition in PEGS and PEGS/PAA@SIRT3 hydrogels. (O–P) Intracellular and mitochondrial ROS assessment of PEGS and PEGS/PAA@SIRT3 hydrogels (n = 3). (Q) Extracellular oxygen content measured using oxygen analyzers (n = 3). (R) Protein level of HIF-1α in BMSCs co-cultured with PEGS or PEGS/PAA@SIRT3 hydrogels (n = 3). (S) ATP production of BMSCs co-cultured with PEGS or PEGS/PAA@SIRT3 hydrogels (n = 3). Data are presented as mean ± standard deviation; $^{*}P < 0.05$, $^{**}P < 0.01$.

due to aging can significantly impair bone regeneration capacity [25]. Initially, the regenerative capacity of bone injuries in adult rats (6 months old) to aged rats (18 months old) was compared by assessing recovery at 4 and 8 weeks following the creation of a critical-size bone defect model. CT reconstructions revealed that adult rats exhibited substantial bone regeneration, recovering approximately 50 % of the bone loss after 8 weeks (Fig. 1A). In contrast, aged rats demonstrated limited bone repair and regeneration, with significantly lower bone volume fraction and bone mineral density compared to adult rats (Fig. 1B–C). Histological analysis through H & E and Masson's trichrome staining revealed impaired bone formation in the cranial defects of aged rats (Fig. 1D–F). Immunofluorescence staining revealed an accumulation of the senescence-associated protein P16 in nascent bone tissue, while osteocalcin (OCN) levels were significantly lower in aged rats (Fig. 1G & S1A-B). Further, using the online database GSE169396, which includes bone tissues from two elderly patients (a 61-year-old female and a 66-year-old male) and two middle-aged patients (a 45-year-old female and a 31-year-old male), single-cell RNA sequencing was performed to investigate the mechanisms underlying the decline in bone reparative capacity due to aging. UMAP dimensionality reduction revealed expression profile similarities across ten cell subclusters: progenitor cells, monocytes, T cells, granulocytes, B cells, dendritic cells (DCs), red blood cells (RBCs), OBs, macrophages, and endothelial cells (ECs) (Fig. 1H–I & S2). Groupwise analysis showed a decrease in the proportion of progenitor cells (18 %–16 %) and OBs (18 %–10 %) in aging bone tissues (Fig. 1J). Enrichment analysis revealed disruptions in cell cycle progression in aged bone, particularly at the G2M checkpoint, alongside increased sensitivity to hypoxic conditions. Moreover, the aging environment impaired collagen formation and extracellular matrix (ECM) synthesis, both of which are essential for BMSC commitment to OB differentiation (Fig. S3). Notably, the analysis identified a significant reduction in the abundance of *Sirt3*-highly expressed (*Sirt3*^{hi}) OB subpopulations with advancing age, suggesting that SIRT3 may play a critical regulatory role in bone formation (Fig. 1K).

Notably, the reduced expression of SIRT3, a critical regulator of osteogenic differentiation through mitochondrial function preservation [26], was observed in the skulls of aged rats. This finding suggests that SIRT3 plays a pivotal role in the mechanisms underlying aging and bone regeneration (Fig. 1L & S1C-D). H_2O_2 is commonly used to accelerate cellular aging and induce senescence *in vitro* by generating oxidative stress, which impairs cell replication and triggers a range of senescence markers [27]. To effectively transfect BMSCs, adeno-associated virus serotype 2 (AAV-2) was employed for SIRT3 transfection (AAV-*Sirt3*) and the preparation of genetically engineered hydrogels (Fig. S4A). Our results indicated that upregulating SIRT3 with AAV-*Sirt3* effectively mitigated H_2O_2-induced senescence in BMSCs, resulting in the downregulation of senescence markers (Fig. S4B). To further investigate the impact of SIRT3 on aging, AAV-*Sirt3* was used to overexpress SIRT3 in BMSCs derived from aged rats. The overexpression of SIRT3 resulted in a significant reduction in senescence markers in these BMSCs, demonstrating remarkable alleviation of the senescence phenotype (Fig. S4C). Nuclear expression of the senescence markers P16 and P21 significantly decreased in senescent BMSCs following treatment with AAV-*Sirt3*, both under oxidative stress-induced senescence (Fig. S5A–B) and natural accumulation of senescence (Fig. S5C–D). Overall, the diminished bone repair capacity observed in senescent BMSCs was partially attributed to the downregulation of SIRT3, while SIRT3 overexpression effectively mitigated the senescence phenotype. SIRT3 plays a pivotal role in alleviating the aging process and promoting bone regeneration, primarily by modulating mitochondrial function and mitigating oxidative stress [28]. SIRT3 can delay the aging of BMSCs induced by advanced glycation end products (AGEs) by promoting mitochondrial autophagy, thereby partially alleviating age-related osteoporosis [29]. Our *in vitro* results also demonstrate that SIRT3 impacts oxidative stress and aging caused by natural accumulation. Additionally, SIRT3 has been shown to protect myocardial cells from oxidative stress during ischemia-reperfusion by translocating to mitochondria under ischemic stress and interacting with SIRT1 to enhance mitochondrial integrity and function [30]. These findings highlight the broad potential of SIRT3 in delaying aging and protecting organ function.

2.2. Preparation and characterization of SIRT3-genetically engineered hypoxia-mimicking hydrogel

The injectable PEGS hydrogel was synthesized through the classical thiol-Michael addition click reaction, followed by the incorporation of inorganic nanoparticles encapsulated with a gene vector (MSN@SIRT3) and grafted carboxyl groups to provide anti-senescent effects and eliminate iron ions (Fig. 2A). The optimal formula was developed by considering key factors such as degradation, mechanical properties, gelation characteristics, AAV encapsulation efficiency, and solution uniformity (Table S2). Analysis of the surface morphology of the hydrogels revealed that all exhibited a porous three-dimensional network structure after freeze-drying (Fig. 2B–C & Table S3). The combination of petite bottle flipping and syringe injection highlighted the commendable injectability of the hydrogel (Fig. 2D). Characterization of the prepolymer structure through red-edge spectroscopy showed a peak at 1635 cm^{-1} corresponding to the extension vibration of the double bond, and a new band at 1566 cm^{-1} in the PEGS-g-PAA polymer corresponding to the stretching vibration of the -COO- group, confirming the successful carboxylation of PEGS-g-PAA. The introduction of mesoporous silica nanoparticles (MSN) resulted in a diminished peak at this position, providing evidence of interaction between the carboxyl group and the aminated MSN (Fig. 2E). Elemental analysis through energy-dispersive X-ray spectroscopy (EDS) revealed the presence of nitrogen and silicon elements in the PEGS/PAA@SIRT3 hydrogel (Fig. 2F). The addition of inorganic components (MSN) significantly enhanced the swelling and tensile mechanical properties of the hydrogels through molecular interactions between the polymer chains and the surface of the inorganic fillers (Fig. 2G–H). Rheological experiments demonstrated that the storage modulus (G′) of the PEGS hydrogel increased over time, surpassing the loss modulus (G″), indicating the eventual formation of a fully cross-linked network. The gelation time, identified by the intersection point of G′ and G″, was found to be less than 30 s (Fig. 2I). Additionally, the energy storage modulus and loss modulus of the hydrogels remained nearly the same within the strain-scanning range of 0.1–100 %, indicating that the hydrogels maintained structural integrity and stability against deformation (Fig. S6A). Regarding the degradation behavior of PEGS and PEGS/PAA@SIRT3 hydrogels, initial swelling led to the precipitation of DTT and borax in PEGS hydrogels, where these components were not fully involved in the reaction. A significant reduction in hydrogel mass was observed due to the rapid release of MSN nanoparticles, which lack hydrogen bonding capability (Fig. 2J). Although the hydrogel remained stable when incubated with PBS *in vitro*, our previous study demonstrated that over 75 % of the hydrogel degraded within three weeks post-implantation *in vivo* [24]. Given that callus formation typically requires approximately four weeks [31,32], the degradation rate of the hydrogel is optimally synchronized with tissue regeneration dynamics, thus promoting optimal bone regeneration. The release rate of AAV-Sirt3-loaded pure PEGS gel (PEGS@SIRT3) was accelerated in PBS buffer, while the drug release kinetics were significantly slowed in the nanocomposite hydrogels (PEGS/PAA@SIRT3), due to the confinement effect provided by the mesoporous structure of MSN (Fig. 2K).

Subsequently, the chelation ability of iron ions and the capacity to induce a hypoxic environment were comprehensively examined for the PEGS/PAA@SIRT3 hydrogel. After immersion in a ferric chloride solution, EDS mapping assays revealed superior iron ion adsorption in the PEGS/PAA@SIRT3 hydrogel (Fig. 2L–M). XPS elemental analysis further confirmed the exceptional efficiency of PEGS/PAA@SIRT3 in capturing iron ions (Fig. 2N & S6B). Cell viability and death staining showed that neither PEGS/PAA nor PEGS/PAA@SIRT3 caused an

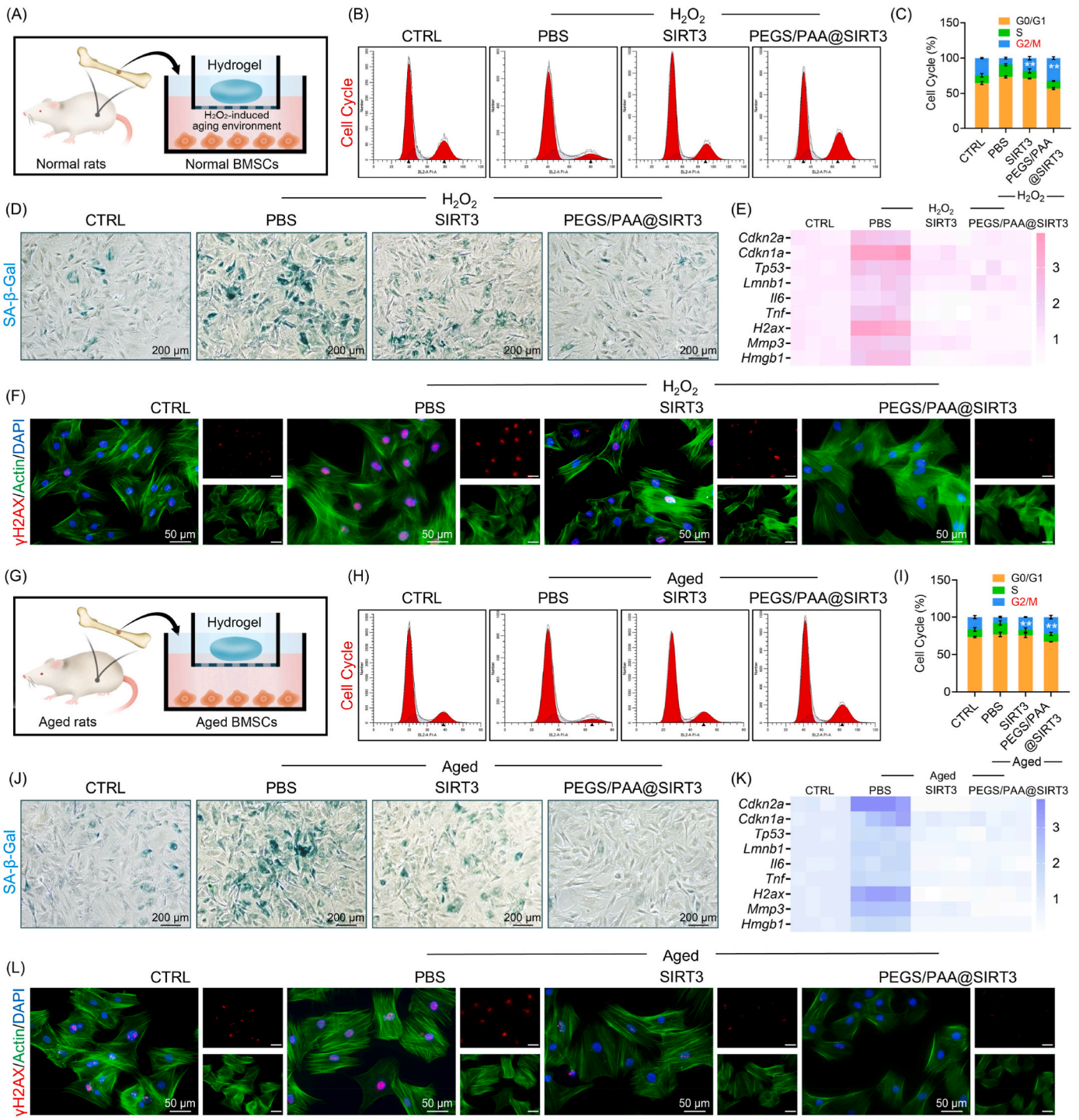

Fig. 3. PEGS/PAA@SIRT3 mitigates the senescence process of BMSCs. (A) Schematic diagram of the extraction and cultivation methods for H_2O_2-treated BMSCs. (B–C) Effect of PEGS/PAA@SIRT3 on the cell cycle in H_2O_2-exposed BMSCs (n = 3). (D) SA-β-Gal staining of H_2O_2-treated BMSCs. (E) Expression levels of SASP-related genes (*Cdkn1a*, *Cdkn2a*, *Tp53*, *Lmnb1*, *Il6*, *Tnf*, *H2ax*, *Mmp3*, and *Hmgb1*) in H_2O_2-exposed BMSCs. (F) Representative immunofluorescence staining images of γH2AX in H_2O_2-treated BMSCs. (G) Schematic diagram of the extraction and cultivation methods for BMSCs derived from aged rats. (H–I) Effect of PEGS/PAA@SIRT3 on the cell cycle in aged BMSCs (n = 3). (J) SA-β-Gal staining of aged BMSCs. (K) Expression levels of SASP-related genes (*Cdkn1a*, *Cdkn2a*, *Tp53*, *Lmnb1*, *Il6*, *Tnf*, *H2ax*, *Mmp3*, and *Hmgb1*) in aged BMSCs. (L) Representative immunofluorescence staining images of γH2AX in aged BMSCs. Data are presented as mean ± standard deviation; $^*P < 0.05$, $^{**}P < 0.01$.

increase in cell death compared to the control (CTRL) group (Fig. S7A–B). Additionally, the CCK8 assay demonstrated that BMSC proliferation was unaffected by either hydrogel, confirming the excellent biocompatibility of PEGS/PAA@SIRT3 (Fig. S7C). In previous studies, both PEGS and PEGS/PAA were implanted *in vivo* for a three-week period, with systematic evaluations of their performance. Results revealed a significantly lower number of infiltrating macrophages (CD68-positive) in the implantation area compared to commercial gelatin, highlighting the superior biosafety of the hydrogels. By the end of week three, the material exhibited a large pore structure (several hundred microns), which promoted tissue integration and stretching [24]. Moreover, PEGS/PAA@SIRT3 demonstrated a significant

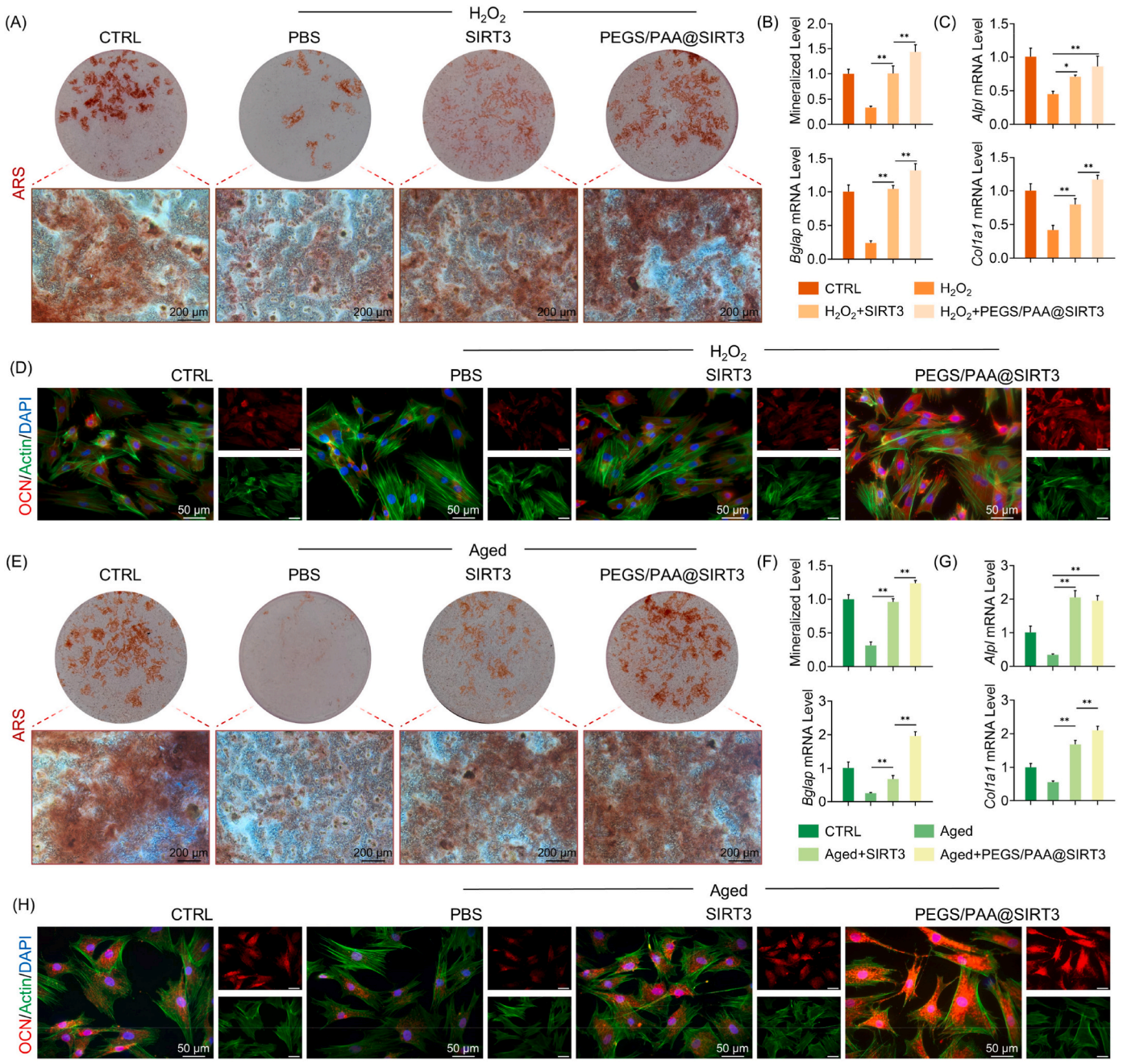

Fig. 4. PEGS/PAA@SIRT3 promotes *in vitro* osteogenic differentiation of BMSCs. (A) Alizarin Red S (ARS) staining of H_2O_2-exposed BMSCs. (B) Quantitative analysis of bone mineral deposition in H_2O_2-exposed BMSCs (n = 3). (C) RT-PCR analysis of osteogenic markers in H_2O_2-exposed BMSCs, including *Alpl*, *Col1a1*, and *Bglap* (n = 4). (D) Immunofluorescence staining of OCN in H_2O_2-exposed BMSCs. (E) ARS staining of aged BMSCs. (F) Quantitative analysis of bone mineral deposition in aged BMSCs (n = 3). (G) RT-PCR analysis of osteogenic markers in aged BMSCs, including *Alpl*, *Col1a1*, and Bglap (n = 4). (H) Immunofluorescence staining of OCN in aged BMSCs. Data are presented as mean ± standard deviation; $^*P < 0.05$, $^{**}P < 0.01$.

reduction in both cellular and mitochondrial superoxide levels (Fig. 2O–P), indicating its effective regulation of the redox status of intracellular and extracellular environments. Importantly, the quantification of oxygen concentration showed that PEGS/PAA@SIRT3 successfully lowered oxygen content in the cellular supernatant (Fig. 2Q). This reduction in oxygen levels was linked to an upregulation of HIF-1α, a core regulator in hypoxic signaling (Fig. 2R). The hypoxic environment created by PEGS/PAA@SIRT3 enhances HIF-1α expression, which has been shown to promote OB proliferation and differentiation, thereby accelerating bone repair [33]. The overexpression of HIF-1α in OBs significantly enhances angiogenesis and bone formation in tensile osteogenesis models, while the absence of HIF-1α impairs these processes, resulting in compromised bone healing [34]. Moreover, the downstream effector gene of HIF-1α, VEGF, plays a dual role in promoting endothelial cell proliferation and migration while modulating osteogenic growth factors to facilitate osteogenesis [35]. Our findings also demonstrated that co-culturing BMSCs with PEGS/PAA@SIRT3 enhanced adenosine triphosphate (ATP) synthesis (Fig. 2S). Hypoxia-induced modulation of energy metabolism helps reduce ROS generation and enhances mitochondrial resilience against hypoxic injury, promoting ATP synthesis in low-oxygen conditions. HIF-1α stabilization promoted glutathione synthesis to maintain redox homeostasis and enhanced glycogen storage to prevent energy deficits, supporting bone cell survival [36]. Furthermore, HIF-1α upregulates

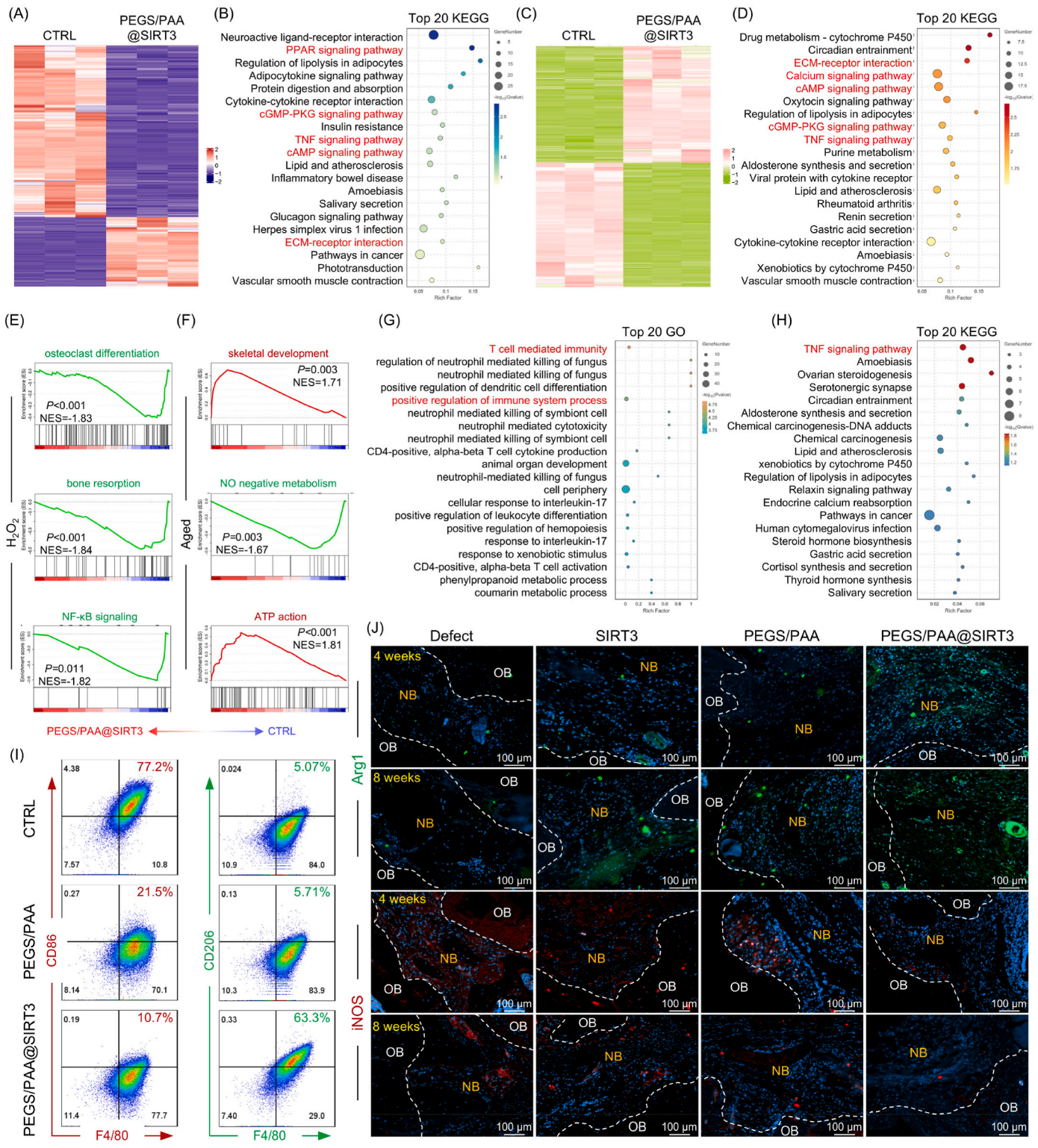

Fig. 5. PEGS/PAA@SIRT3 regulates bone metabolism and immune processes. (A) Heat map illustrating differentially expressed genes following PEGS/PAA@SIRT3 intervention in hydrogen peroxide-induced aging BMSCs. (B) Bubble plots highlighting the top 20 signaling pathways exhibiting the most significant alterations due to PEGS/PAA@SIRT3 intervention in hydrogen peroxide-induced aging BMSCs. (C) Heat map depicting differentially expressed genes resulting from PEGS/PAA@SIRT3 intervention in naturally aging BMSCs. (D) Bubble plots showcasing the top 20 signaling pathways with the most notable changes following PEGS/PAA@SIRT3 intervention in naturally aging BMSCs. (E) Gene Set Enrichment Analysis (GSEA) of key pathways affected by PEGS/PAA@SIRT3 intervention in hydrogen peroxide-induced aging BMSCs, including pathways related to osteoblast differentiation, regulation of bone resorption, and NF-κB-related signaling. (F) GSEA of critical pathways influenced by PEGS/PAA@SIRT3 intervention in naturally aging BMSCs, encompassing pathways involved in embryonic skeletal joint development, intracellular estrogen receptor activity, negative regulation of nitric oxide metabolism, and ATP-related signaling. (G–H) Bubble plot illustrating the top 20 signaling pathways that displayed consistent alterations following PEGS/PAA@SIRT3 intervention in senescent cells induced by different aging models. (I) Immune profiling of M1 and M2 macrophage polarization *via* flow cytometry analysis. (J) Immunofluorescent staining of iNOS (a marker of M1 macrophage activation) and Arg1 (a marker of M2 macrophage polarization). Data are presented as mean ± standard deviation; $^{*}P < 0.05$, $^{**}P < 0.01$.

glycolysis in the bone marrow microenvironment by increasing pyruvate dehydrogenase kinase 1 (PDK1), which supports OB differentiation [37] and angiogenesis [38]. HIF-1α is upregulated during BMSC differentiation, facilitating glycolysis to supply the necessary energy for BMSC proliferation and modulating bone homeostasis by regulating energy metabolism [39]. Consequently, an injectable hydrogel with exceptional physical and chemical properties that sequesters free iron ions was developed, thereby creating a hypoxic microenvironment that promotes osteogenesis.

2.3. The genetically modified hydrogel combated cellular senescence induced by H_2O_2 and natural aging

To thoroughly investigate the effects of genetically modified hydrogel on cellular senescence, experiments were performed using two distinct models: *in vitro* H_2O_2-induced BMSCs (Fig. 3A) and BMSCs from aged rats *in vivo* (Fig. 3G). The percentage of cells in the G2/M phase indicates mitotic activity, with a reduced mitotic capacity in SCs, reflected by a lower proportion of cells in the G2/M phase [40]. Both H_2O_2-induced senescent BMSCs and BMSCs from senescent rats exhibited a significant decrease in the G2/M phase cell population (Fig. 3B and H). However, treatment with SIRT3 and PEGS/PAA@SIRT3 enhanced mitotic capacity (Fig. 3C and I). Senescence-associated beta-galactosidase (SA-β-gal) is an enzyme capable of hydrolyzing galactose linkages [41]. While activity remains low in normal cells, it is markedly upregulated in SCs. SIRT3 overexpression reversed the age-related increase in SA-β-gal positive cells (Fig. 3D and J & S8A). PCR analysis revealed that SIRT3 and PEGS/PAA@SIRT3 interventions effectively reduced the SASP, including *Cdkn1a*, *Cdkn2a*, *Tp53*, *Lmnb1*, *Il6*, *Tnf*, *H2ax*, *Mmp3*, and *Hmgb1* (Fig. 3E and K). Notably, PEGS/PAA@SIRT3 exhibited a more significant effect on the DNA damage marker *H2ax* compared to other molecules, as confirmed by immunofluorescence staining (Fig. 3F and L & S8B). SIRT3 preserves mitochondrial function and integrity by deacetylating key enzymes and proteins within the mitochondria, including isocitrate dehydrogenase 2 (IDH2), thus mitigating oxidative stress-induced cellular damage [42]. Given that oxidative damage is a primary driver of aging, SIRT3's enhanced antioxidant capacity suggests its potential in alleviating age-related decline [43]. SIRT3 plays a pivotal role in regulating mitochondrial energy metabolism and enhancing ATP production, thereby promoting the expression and activity of respiratory chain proteins [8]. Notably, the therapeutic efficacy of PEGS/PAA@SIRT3 exceeded that of SIRT3 alone, likely due to the enhanced activation of PEGS/PAA hydrogel within the hypoxic microenvironment. Hypoxia activates the HIF-1 signaling pathway, which regulates the expression of antioxidant genes such as superoxide dismutase (SOD), glutathione peroxidase (GPX), and catalase (CAT) [44]. These antioxidant enzymes effectively neutralize free radicals and other oxidizing agents, mitigating oxidative damage and slowing the aging process [45]. Additionally, the HIF-1α pathway modulates intracellular iron levels and limits free iron generation, thereby preventing ferroptosis-related cellular damage [46]. Together, PEGS/PAA@SIRT3 effectively alleviated cellular senescence induced by oxidative stress or natural aging.

2.4. The genetically engineered hydrogel facilitated the lineage commitment of BMSCs towards OBs

The diminished osteogenic capacity of aging BMSCs prompted the use of SIRT3 overexpression to assess its impact on osteogenic differentiation. Alkaline phosphatase (ALP) expression is elevated during the early phase of osteogenesis, while OCN and collagen type I (COL I) serve as markers of advanced differentiation. AAV-*Sirt3* enhanced the expression of osteogenic markers in normal BMSCs, H_2O_2-induced senescent BMSCs, and BMSCs from aged rats (Fig. S9A–B). Treatment with SIRT3 and PEGS/PAA@SIRT3 further revealed that aging impaired early osteogenic differentiation, as indicated by ALP staining, but upregulation of SIRT3 significantly increased ALP expression (Fig. S10A–B). Alizarin red staining (ARS) showed a marked reduction in calcium nodules in SCs, suggesting impaired bone mineralization due to aging (Fig. 4A–B). However, SIRT3 treatment restored calcium nodule formation in BMSCs (Fig. 4E–F). PCR analysis demonstrated that SIRT3 overexpression effectively reversed the age-associated decline in osteogenic markers, including *Alpl*, *Col1a1*, and *Bglap* (Fig. 4C and G). Additionally, OCN, a late osteogenesis marker, exhibited a consistent decrease with aging, which was restored by SIRT3 overexpression (Fig. 4D and H). Notably, PEGS/PAA@SIRT3 had a more significant impact on osteogenic restoration than SIRT3 alone, likely due to its activation of a hypoxic microenvironment [47]. The hypoxia induced by PEGS/PAA hydrogel activates the 5′-AMP-activated protein kinase (AMPK) signaling pathway [48], an energy-sensing pathway that regulates cellular metabolism and provides protection in response to hypoxia [49]. Under hypoxic conditions, AMPK is activated, leading to enhanced glucose uptake and oxidation, improved mitochondrial respiration, and increased ATP synthesis, all of which accelerate osteogenesis [50]. In summary, the integration of SIRT3-activated cellular potential with the supportive environment provided by PEGS/PAA enabled PEGS/PAA@SIRT3 to promote osteogenic differentiation. Modulating the microenvironment to enhance osteogenesis is increasingly recognized as a promising strategy for improving bone healing. A stratified hydrogel system with immune-responsive properties adapts to the bone regeneration environment and facilitates mitochondrial-targeted transfer between cells. Sustained mitochondrial delivery from macrophages can restore BMSC bioenergetics, addressing the energy deficits caused by local inflammation [51]. This approach, which simultaneously modulates the microenvironment and enhances energy production, aligns with the core concept of our study.

2.5. The genetically modified hydrogel counteracted senescence to enhance osteogenesis via regulating immune signaling

To further elucidate the mechanisms by which genetically modified hydrogel enhances age-related osteogenic differentiation, BMSCs co-cultured with the hydrogel under H_2O_2-induced or naturally aging conditions were subjected to RNA sequencing analysis. The results revealed significant expression changes in 604 genes following PEGS/PAA@SIRT3 treatment compared to H_2O_2 treatment (Fig. 5A & S11A), and 466 genes compared to aging BMSCs (Fig. 5C & S11B). The activation of the cyclic adenosine monophosphate (cAMP) pathway has been shown to significantly enhance osteogenic differentiation in stem cells [52]. By activating protein kinase A (PKA) and regulating transcription factors like cAMP response element-binding protein (CREB), this pathway promotes the expression of genes associated with osteogenic differentiation (Fig. 5B and D & S12-13). Our study focused on genes related to osteogenic differentiation, senescence, and hypoxia (Fig. S14). Although the specific target genes influenced by PEGS/PAA@SIRT3 varied between the two cell lines, all demonstrated significant protective effects. GSEA analysis revealed that PEGS/PAA@SIRT3 had a strong inhibitory effect on osteoclastogenesis-related pathways. Aging is characterized by a decline in energy metabolism and differentiation capacity [53], but PEGS/PAA@SIRT3 treatment notably activated ATP synthesis and bone formation-related pathways (Fig. 5E–F). Furthermore, 107 genes were consistently altered in both comparisons (Fig. S15A). The receptor for advanced glycation end products (*Ager*) is a key receptor protein that binds to AGEs and plays a critical role in regulating inflammation and immune responses [54]. In bone immunity, *Ager* is crucial in modulating the functions of bone marrow macrophages and osteoclasts, where its activation increases bone resorption (Fig. S15B). The transcription factor *Nfatc2* is essential for regulating immune cell activation, facilitating osteoclast differentiation, and enhancing their activity upon stimulation [55]. According to the enrichment analysis, PEGS/PAA@SIRT3 treatment induced significant changes in a variety of bone immune-related factors, thereby accelerating bone regeneration (Fig. 5G–H).

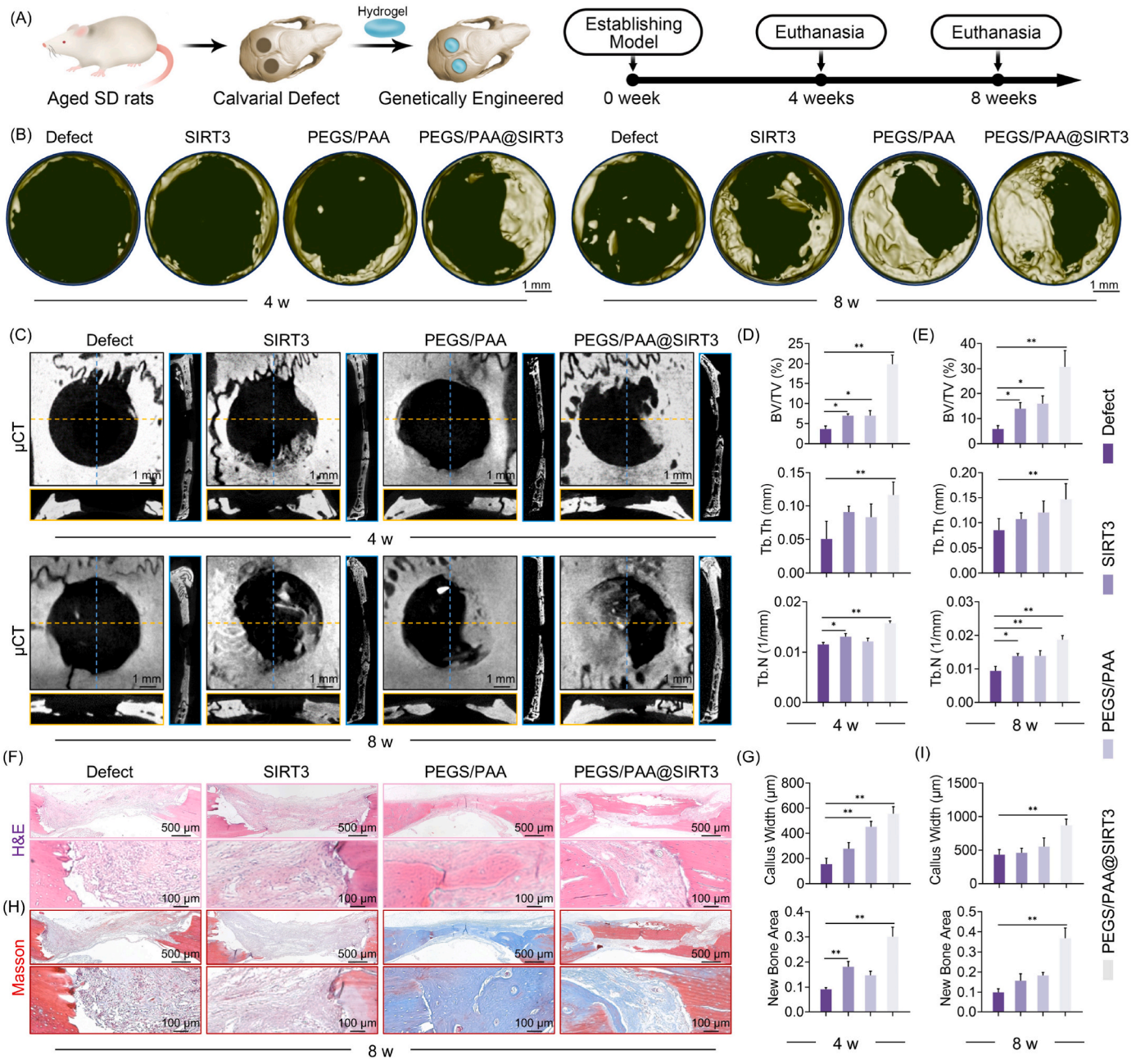

Fig. 6. Evaluation of bone regeneration in critical-sized calvarial defects at 4 and 8 weeks. (A) Schematic of model construction and specimen collection. (B–C) New bone formation in the calvarial defect evaluated using micro-CT imaging and 3D reconstruction at 4 weeks and 8 weeks. (D) Quantitative analysis of bone volume ratio (BV/TV), trabecular thickness (Tb.Th), and trabecular number (Tb.N) in the samples at 4 weeks (n = 3). (E) Quantitative analysis of BV/TV, Tb.Th, and Tb.N in the samples at 8 weeks (n = 3). (F–G) Representative H & E images of the defect area and callus width (n = 3). (H–I) Representative MTS images of the defect area and new bone area (n = 3). Data are presented as mean ± standard deviation; $^{*}P < 0.05$, $^{**}P < 0.01$.

Consequently, the impact of PEGS/PAA@SIRT3 on macrophage polarization was investigated. Flow cytometry results showed that PEGS/PAA@SIRT3 significantly promoted M2 macrophage polarization and inhibited M1 macrophage polarization (Fig. 5I & S16A-B). Additionally, both *in vitro* and *in vivo* double immunofluorescent labeling confirmed the shift of macrophages from a proinflammatory to an anti-inflammatory phenotype induced by PEGS/PAA@SIRT3 (Fig. 5J & S17A-D). Overall, PEGS/PAA@SIRT3 effectively alleviated senescence and promoted osteogenesis through the modulation of immune signaling associated with macrophage polarization [56]. Hydrogels infused with magnesium have been shown to enhance osteoporotic bone repair by releasing hydrogen, which scavenges ROS and modulates immune responses [57]. Moreover, multibioactive nanotherapies using self-assembled nanomicelles not only promote osteogenic differentiation of stem cells but also improve the bone immune environment, demonstrating superior bone regeneration potential [58]. Our PEGS/PAA@SIRT3 hydrogel has been shown to effectively modulate the immune microenvironment, indicating its broader role and multiple regulatory mechanisms in promoting osteogenesis.

2.6. *The genetically engineered hydrogel expedited bone regeneration in a calvarial defect model of aged rats*

To assess the efficacy of PEGS/PAA@SIRT3 in mitigating aging and promoting bone regeneration in elderly individuals, a critical-size bone defect model was established in aged rats (Fig. 6A). CT reconstruction

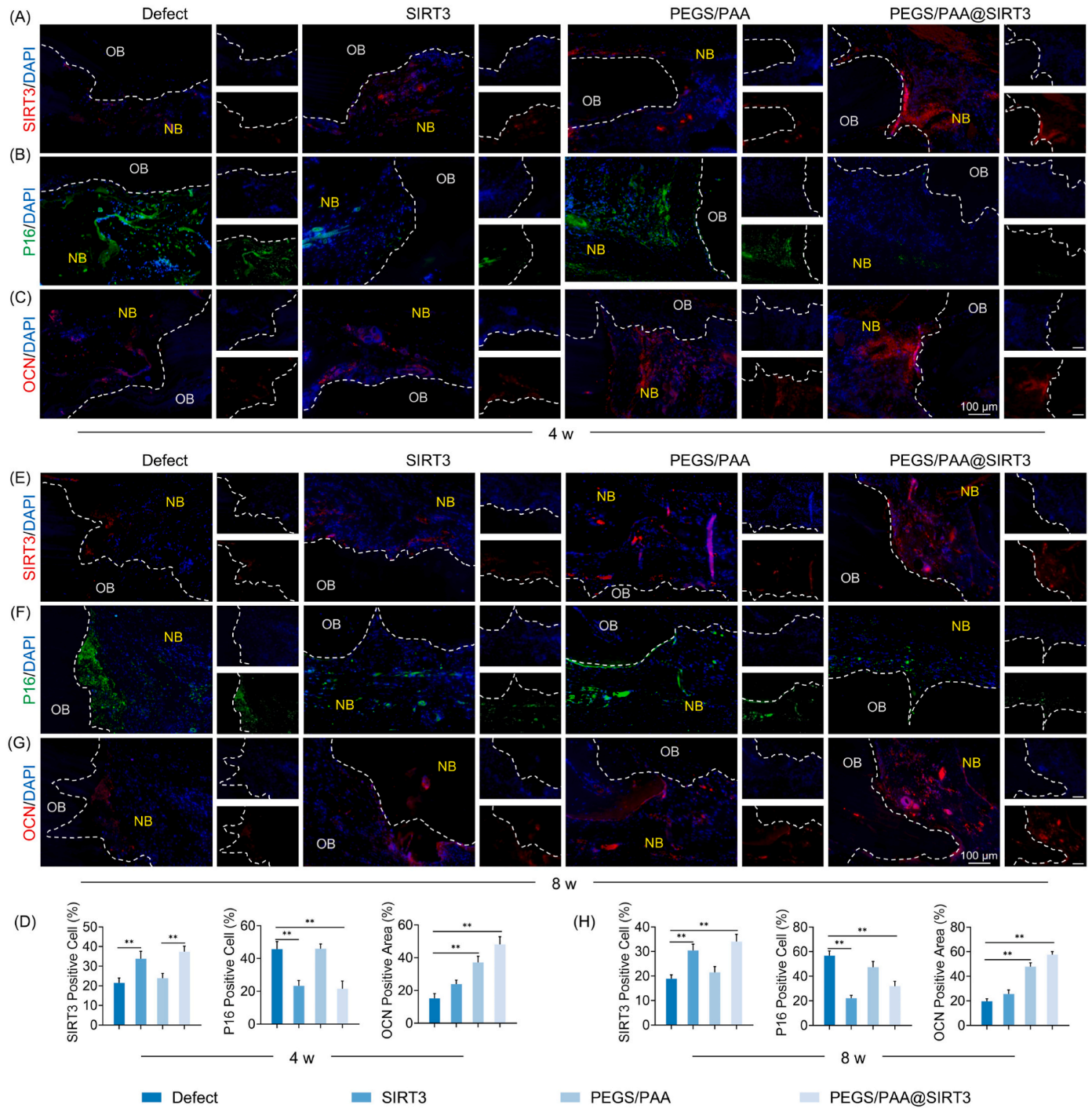

Fig. 7. PEGS/PAA@SIRT3 protects bone formation and alleviates the aging process by activating SIRT3. (A) Representative immunofluorescence staining images of SIRT3 at 4 weeks. (B) Representative immunofluorescence staining images of P16 at 4 weeks. (C) Representative immunofluorescence staining images of OCN at 4 weeks. (D) Quantitative analysis of SIRT3, P16, and OCN at 4 weeks (n = 3). (E) Representative immunofluorescence staining images of SIRT3 at 8 weeks. (F) Representative immunofluorescence staining images of P16 at 8 weeks. (G) Representative immunofluorescence staining images of OCN at 8 weeks. (H) Quantitative analysis of SIRT3, P16, and OCN at 8 weeks (n = 3). Data are presented as mean ± standard deviation; $^{*}P < 0.05$, $^{**}P < 0.01$. New bone (NB) and original bone (OB).

analysis at 4 and 8 weeks revealed minimal new bone formation in the Defect group, indicating a significant decline in bone regenerative capacity (Fig. 6B–C). Aged rats treated solely with SIRT3 showed limited new bone formation, though a significant increase in bone volume fraction (BV/TV) was observed compared to the Defect group (Fig. 6D). By the eighth week, significant new bone formation was observed in the cranial defects of aging rats, attributed to the enhanced connectivity of the hydrogels and their ability to mimic a hypoxic microenvironment (Fig. 6E). PEGS/PAA@SIRT3 promoted bone regeneration more effectively than other treatments, with nearly half of the bone defect area covered by new bone at 8 weeks (Fig. 6F). H & E staining differentiated bone tissue from cells, while Masson's trichrome staining revealed that mature bone stained red, new bone was red, and collagen appeared blue (Fig. 6G). At 4 weeks post-surgery, fibrous connections were observed at the bone defects in the Defect group, while both the SIRT3 and PEGS/PAA groups displayed light blue collagen deposits. Notably, the PEGS/

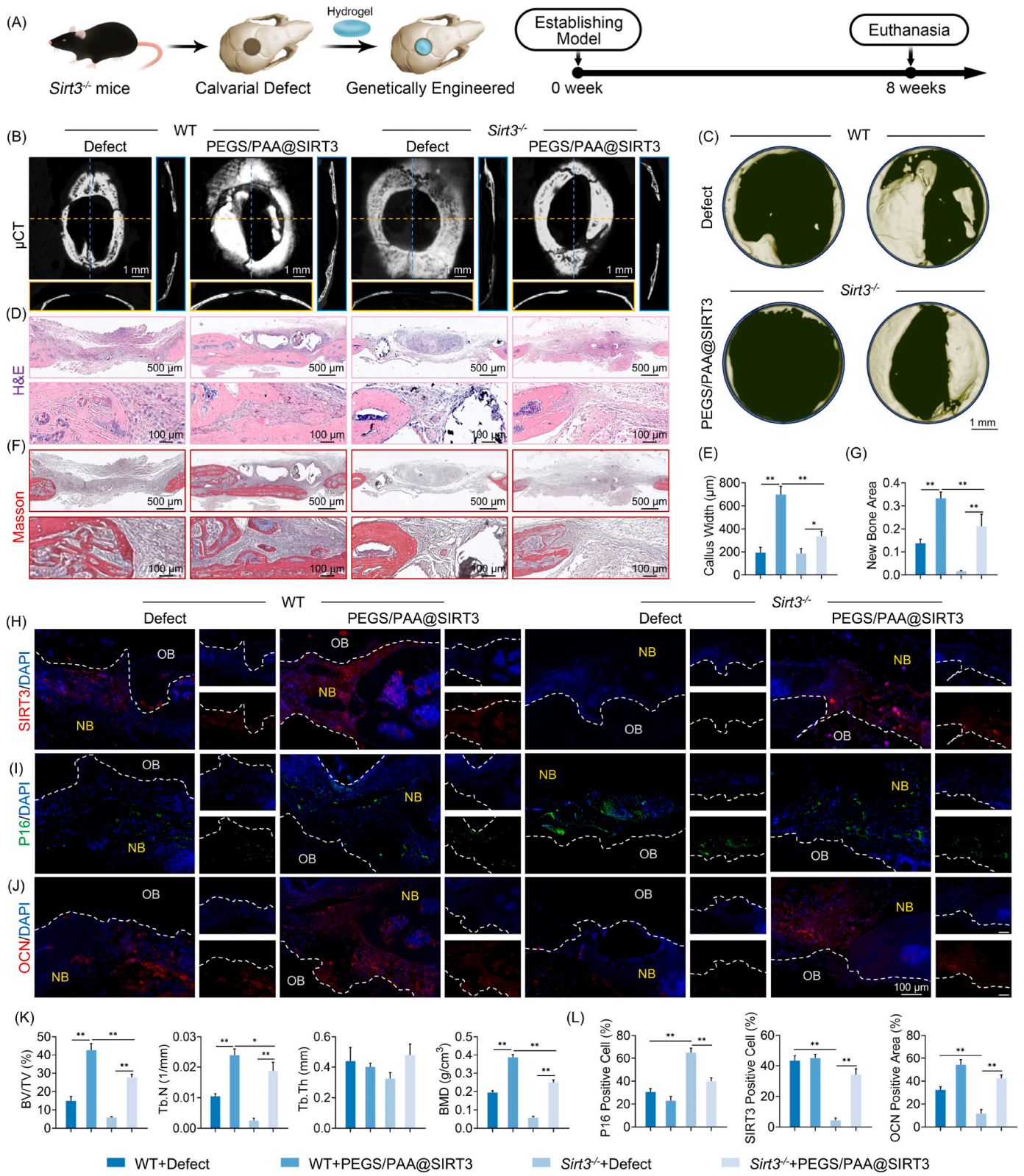

Fig. 8. PEGS/PAA@SIRT3 restores impaired bone regeneration in *Sirt3*-deficient mice. (A) Schematic of model construction and specimen collection. (B–C) New bone formation evaluated by micro-CT imaging and 3D reconstruction in WT and *Sirt3*$^{-/-}$ mice. (D–E) Representative H & E images of the defect area and callus width in WT and *Sirt3*$^{-/-}$ mice (n = 3). (F–G) Representative MTS images of the defect area and new bone area in WT and *Sirt3*$^{-/-}$ mice (n = 3). (H–J) Representative immunofluorescence staining images of SIRT3, P16, and OCN. (K) Quantitative analysis of bone volume ratio (BV/TV), trabecular thickness (Tb.Th), trabecular number (Tb.N), and bone mineral density (BMD) in WT and *Sirt3*$^{-/-}$ mice (n = 3). (L) Quantitative analysis of SIRT3, P16, and OCN in WT and *Sirt3*$^{-/-}$ mice (n = 3). Data are presented as mean ± standard deviation; *$P < 0.05$, **$P < 0.01$. New bone (NB) and original bone (OB).

PAA@SIRT3 group exhibited new bone formation characterized by red and blue hues (Fig. S18A). At 8 weeks post-transplantation, the PEGS/PAA@SIRT3 group showed mature red bone development, indicating successful restoration of bone continuity and suggesting that PEGS/PAA@SIRT3 treatment expedited bone healing (Fig. 6H–I & S18B). Immunofluorescence staining revealed that exogenous SIRT3 significantly increased SIRT3 levels at the bone defect site (Fig. 7A), resulting in a reduction of the aging marker P16 expression (Fig. 7B–D). Notably, while the PEGS/PAA hydrogel alone did not significantly affect P16 expression, it enhanced the positive area of OCN compared to the defect group (Fig. 7E–G). In addition to promoting osteogenesis, PEGS/PAA may exert other biological effects that contribute to bone healing (Fig. 7H). HIF-1α expression was significantly observed in the *de novo* bone tissue in both PEGS/PAA and PEGS/PAA@SIRT3 hydrogels during both early and late stages of the repair process (Fig. S19A–B). Moreover, H & E staining of major organs such as the heart, liver, spleen, lungs, and kidneys revealed no evidence of *in vivo* toxicity (Fig. S20). Activation of HIF-1α by PEGS/PAA has been shown to promote angiogenesis, thereby facilitating the delivery of essential nutrients and oxygen for bone tissue regeneration [59]. Additionally, HIF-1α acts as a critical mediator linking angiogenesis and glycolysis by regulating the transcriptional activation of pyruvate kinase 2 (PKM2) [60]. However, the bone defect site supplemented with exogenous SIRT3 alone did not show a significant increase in OCN accumulation, likely due to the lack of sustained-release carriers that provide extended efficacy and promote bone connectivity. Thus, PEGS/PAA@SIRT3 enhanced the process of bone repair and regeneration, even in the context of aging. The difficulty of bone tissue repair associated with aging or inflammation can impair regenerative capacity, affecting both the function and quantity of bone cells and hindering the bone healing process [61]. Combined photothermal therapy and on-demand drug release have been shown to be effective strategies for diabetic bone regeneration, underscoring the advantages of a combined system that integrates biophysical and biochemical cues [62,63]. Therefore, a comprehensive and multifaceted treatment strategy is essential for patients with bone defects and comorbid conditions.

2.7. Bone regeneration driven by genetically engineered hydrogel relied on the activation of SIRT3 in vivo

To investigate the regulatory role of SIRT3 in aging and bone regeneration, global knockout mice (*Sirt3*$^{-/-}$) were generated as previously described [8]. PEGS/PAA@SIRT3 were surgically implanted into cranial defects of both wild-type (WT) and *Sirt3*$^{-/-}$ mice (Fig. 8A). The results showed that PEGS/PAA@SIRT3 treatment accelerated cranial defect regeneration in WT mice (Fig. 8B–C & K). In contrast, the absence of SIRT3 in *Sirt3*$^{-/-}$ mice resulted in a reduced capacity for self-healing in the skull, with minimal new bone formation observed (Fig. 8D–G). This discrepancy likely arises from the inability of exogenous SIRT3 to fully compensate for the lack of endogenous SIRT3. Notably, the administration of exogenous SIRT3 *via* PEGS/PAA@SIRT3 increased SIRT3 expression in the cranial region of both WT and *Sirt3*$^{-/-}$ mice (Fig. 8H). The deletion of SIRT3 led to an upregulation of the aging biomarker P16 and a downregulation of the osteogenic marker OCN in the murine skull, which was reversed by the exogenous supplementation of SIRT3 (Fig. 8I–J & L). These findings further support the role of SIRT3 in promoting bone regeneration by inhibiting the aging process *in vivo*. In aging stem cells, mitochondrial homeostasis is disrupted, accompanied by changes in epigenetic regulation, including altered DNA methylation, histone modifications, and heterochromatin organization [64]. As a deacetylase, SIRT3 regulates epigenetic factors to maintain chromatin stability, thus delaying BMSC aging [65]. Numerous studies have shown that SIRT3 enhances intracellular antioxidant capacity by deacetylating SOD2, promoting osteogenesis [66]. Additionally, ROS-induced osteoclastogenesis is suppressed by SIRT3-activated SOD2, which effectively scavenges ROS and indirectly inhibits osteoclastogenesis [67]. In summary, exogenous supplementation of SIRT3 *via* hypoxia-mimicking hydrogels enhanced bone remodeling, even in the absence of endogenous SIRT3.

3. Conclusion

Given the compromised cellular conditions and deteriorated ECM in aging environments, a dual-functional genetically engineered hydrogel was developed, which not only rejuvenated senescent BMSCs by scavenging SASPs but also created a hypoxic microenvironment through ion chelation, effectively implementing an “inside-out” strategy to enhance bone regeneration in the elderly. At the cellular level, overexpression of SIRT3 was linked to enhanced osteogenic potential and reduced age-related damage in BMSCs, acting as an intrinsic regulatory mechanism. At the extracellular level, carboxyl groups within the PEGS/PAA structure chelate iron ions, simulating hypoxic conditions *via* HIF-1α activation, representing an extrinsic modulatory effect. The coordinated anti-aging and pro-osteogenic effects were mechanistically driven by maintaining bone immune homeostasis. Notably, the *in vivo* cranial defect model in aged rats and *Sirt3* knockout mice demonstrated a significant enhancement in bone formation, with this beneficial effect attributed to the activation of endogenous SIRT3 signaling. In conclusion, the genetically engineered hydrogel developed in this study shows immense potential for practical applications in enhancing senile bone regeneration, offering promising prospects for clinical translation in addressing complex bone injuries.

CRediT authorship contribution statement

Yanrun Zhu: Validation, Methodology, Data curation, Conceptualization. **Lili Sun:** Formal analysis, Data curation, Conceptualization. **Mingzhuang Hou:** Writing – original draft, Visualization, Data curation, Conceptualization. **Jianfeng Yu:** Formal analysis, Conceptualization. **Chenqi Yu:** Methodology, Investigation. **Zihan Zhang:** Visualization, Validation. **Huilin Yang:** Supervision, Conceptualization. **Changsheng Liu:** Methodology, Investigation. **Lixin Huang:** Formal analysis. **Dinghua Jiang:** Supervision, Formal analysis. **Yijian Zhang:** Writing – review & editing, Supervision, Conceptualization. **Yuan Yuan:** Writing – review & editing, Visualization, Supervision. **Xuesong Zhu:** Writing – review & editing, Visualization, Supervision, Funding acquisition.

Ethics approval and consent to participate

Animal protocols were approved by the Ethics Committee of Soochow University (SUDA20230906A02).

Data Availability Statement

The data that support the findings of this study are available from the corresponding author upon reasonable request.

Declaration of competing interest

None.

Acknowledgements

This research was supported by grants from the National Natural Science Foundation of China (82272494, 82472452, 82402864), the National Key R & D Program of China (2022YFC2502902), the Key Project of Jiangsu Health Commission (K2023079), the Natural Science Foundation of Jiangsu Province (BK20240368), the Basic Research Pilot Project Suzhou (SSD2024062), the China Postdoctoral Science Foundation (2024M762313), the Boxi Youth Natural Science Foundation (BXQN2023014), the Postgraduate Research & Practice Innovation

Program of Jiangsu Province (KYCX24_3337), and the Priority Academic Program Development of Jiangsu Higher Education Institutions (PAPD).

Appendix A. Supplementary data

Supplementary data to this article can be found online at https://doi.org/10.1016/j.bioactmat.2025.05.003.

References

[1] L. Tong, A.J.v. Wijnen, H. Wang, D. Chen, Advancing bone biology: the mutual promotion of biology and pioneering technologies, Innov.Life 2 (3) (2024) 100078.

[2] L. Xie, G. Wang, Y. Wu, Q. Liao, S. Mo, X. Ren, L. Tong, W. Zhang, M. Guan, H. Pan, P.K. Chu, H. Wang, Programmed surface on poly(aryl-ether-ether-ketone) initiating immune mediation and fulfilling bone regeneration sequentially, Innovation 2 (3) (2021) 100148.

[3] W. Liang, Q. Chen, S. Cheng, R. Wei, Y. Li, C. Yao, Z. Ouyang, D. Kang, A. Chen, Z. Liu, K. Li, X. Bai, Q. Li, B. Huang, Skin chronological aging drives age-related bone loss via secretion of cystatin-A, Nature Aging 2 (10) (2022) 906–922.

[4] M.M. Gonzales, V.R. Garbarino, T.F. Kautz, J.P. Palavicini, M. Lopez-Cruzan, S. K. Dehkordi, J.J. Mathews, H. Zare, P. Xu, B. Zhang, C. Franklin, M. Habes, S. Craft, R.C. Petersen, T. Tchkonia, J.L. Kirkland, A. Salardini, S. Seshadri, N. Musi, M. E. Orr, Senolytic therapy in mild Alzheimer's disease: a phase 1 feasibility trial, Nat. Med. 29 (10) (2023) 2481–2488.

[5] Y. Wang, L. Che, X. Chen, Z. He, D. Song, Y. Yuan, C. Liu, Repurpose dasatinib and quercetin: targeting senescent cells ameliorates postmenopausal osteoporosis and rejuvenates bone regeneration, Bioact. Mater. 25 (2023) 13–28.

[6] W. Li, J. Lai, Y. Zu, P. Lai, Cartilage-inspired hydrogel lubrication strategy, Innovation 3 (5) (2022) 100275.

[7] B. Yu, J. Liu, J. Cheng, L. Zhang, C. Song, X. Tian, Y. Fan, Y. Lv, X. Zhang, A static magnetic field improves iron metabolism and prevents high-fat-diet/streptozocin-induced diabetes, Innovation 2 (1) (2021) 100077.

[8] Y. Zhang, Y. Liu, M. Hou, X. Xia, J. Liu, Y. Xu, Q. Shi, Z. Zhang, L. Wang, Y. Shen, H. Yang, F. He, X. Zhu, Reprogramming of mitochondrial respiratory chain complex by targeting SIRT3-COX4I2 Axis attenuates osteoarthritis progression, Adv. Sci. (Weinh.) 10 (10) (2023) e2206144.

[9] K. Zheng, J. Bai, N. Li, M. Li, H. Sun, W. Zhang, G. Ge, X. Liang, H. Tao, Y. Xue, Y. Hao, C. Zhu, Y. Xu, D. Geng, Protective effects of sirtuin 3 on titanium particle-induced osteogenic inhibition by regulating the NLRP3 inflammasome via the GSK-3β/β-catenin signalling pathway, Bioact. Mater. 6 (10) (2021) 3343–3357.

[10] Y. Li, Y. Xiao, C. Liu, The horizon of materiobiology: a perspective on material-guided cell behaviors and tissue engineering, Chem. Rev. 117 (5) (2017) 4376–4421.

[11] Y. Yu, S. Wang, X. Chen, Z. Gao, K. Dai, J. Wang, C. Liu, Sulfated oligosaccharide activates endothelial Notch for inducing macrophage-associated arteriogenesis to treat ischemic diseases, Proc. Natl. Acad. Sci. U. S. A. 120 (46) (2023) e2307480120.

[12] G. Yuan, X. Lin, Y. Liu, M.B. Greenblatt, R. Xu, Skeletal stem cells in bone development, homeostasis, and disease, Protein Cell 15 (8) (2024) 559–574.

[13] A. Petersen, A. Princ, G. Korus, A. Ellinghaus, H. Leemhuis, A. Herrera, A. Klaumünzer, S. Schreivogel, A. Woloszyk, K. Schmidt-Bleek, S. Geissler, I. Heschel, G.N. Duda, A biomaterial with a channel-like pore architecture induces endochondral healing of bone defects, Nat. Commun. 9 (1) (2018) 4430.

[14] Y. Xu, Y. Li, A. Gao, P.K. Chu, H. Wang, Gasotransmitter delivery for bone diseases and regeneration, Innov.Life 1 (1) (2023) 100015.

[15] S. Stegen, K. Laperre, G. Eelen, G. Rinaldi, P. Fraisl, S. Torrekens, R. Van Looveren, S. Loopmans, G. Bultynck, S. Vinckier, F. Meersman, P.H. Maxwell, J. Rai, M. Weis, D.R. Eyre, B. Ghesquière, S.M. Fendt, P. Carmeliet, G. Carmeliet, HIF-1α metabolically controls collagen synthesis and modification in chondrocytes, Nature 565 (7740) (2019) 511–515.

[16] B. Galy, M. Conrad, M. Muckenthaler, Mechanisms controlling cellular and systemic iron homeostasis, Nat. Rev. Mol. Cell Biol. 25 (2) (2024) 133–155.

[17] C.V. Maduka, A.V. Makela, A. Tundo, E. Ural, K.B. Stivers, M.M. Kuhnert, M. Alhaj, E. Hoque Apu, N. Ashammakhi, K.D. Hankenson, R. Narayan, J.H. Elisseeff, C. H. Contag, Regulating the proinflammatory response to composite biomaterials by targeting immunometabolism, Bioact. Mater. 40 (2024) 64–73.

[18] C. Li, F. Sun, J. Tian, J. Li, H. Sun, Y. Zhang, S. Guo, Y. Lin, X. Sun, Y. Zhao, Continuously released Zn(2+) in 3D-printed PLGA/β-TCP/Zn scaffolds for bone defect repair by improving osteoinductive and anti-inflammatory properties, Bioact. Mater. 24 (2023) 361–375.

[19] M. Dziadek, K. Dziadek, K. Checinska, B. Zagrajczuk, M. Golda-Cepa, M. Brzychczy-Wloch, E. Menaszek, A. Kopec, K. Cholewa-Kowalska, PCL and PCL/bioactive glass biomaterials as carriers for biologically active polyphenolic compounds: comprehensive physicochemical and biological evaluation, Bioact. Mater. 6 (6) (2021) 1811–1826.

[20] A. Patel, A.K. Gaharwar, G. Iviglia, H. Zhang, S. Mukundan, S.M. Mihaila, D. Demarchi, A. Khademhosseini, Highly elastomeric poly(glycerol sebacate)-co-poly(ethylene glycol) amphiphilic block copolymers, Biomaterials 34 (16) (2013) 3970–3983.

[21] S. Huo, X. Tang, W. Chen, D. Gan, H. Guo, Q. Yao, R. Liao, T. Huang, J. Wu, J. Yang, G. Xiao, X. Han, Epigenetic regulations of cellular senescence in osteoporosis, Ageing Res. Rev. (2024) 102235.

[22] Z. He, C. Sun, Y. Ma, X. Chen, Y. Wang, K. Chen, F. Xie, Y. Zhang, Y. Yuan, C. Liu, Rejuvenating aged bone repair through multihierarchy reactive oxygen species-regulated hydrogel, Adv. Mater. 36 (9) (2024) e2306552.

[23] Y. Wang, C. Wan, L. Deng, X. Liu, X. Cao, S.R. Gilbert, M.L. Bouxsein, M.C. Faugere, R.E. Guldberg, L.C. Gerstenfeld, V.H. Haase, R.S. Johnson, E. Schipani, T. L. Clemens, The hypoxia-inducible factor alpha pathway couples angiogenesis to osteogenesis during skeletal development, J. Clin. Investig. 117 (6) (2007) 1616–1626.

[24] L. Sun, Y. Ma, H. Niu, Y. Liu, Y. Yuan, C. Liu, Recapitulation of in situ endochondral ossification using an injectable hypoxia-mimetic hydrogel, Adv. Funct. Mater. 31 (5) (2021) 2008515.

[25] K. Dai, Z. Geng, W. Zhang, X. Wei, J. Wang, G. Nie, C. Liu, Biomaterial design for regenerating aged bone: materiobiological advances and paradigmatic shifts, Natl. Sci. Rev. 11 (5) (2024) nwae076.

[26] P. Dashti, E.A. Lewallen, J.A.R. Gordon, M.A. Montecino, J.R. Davie, G.S. Stein, J. van Leeuwen, B.C.J. van der Eerden, A.J. van Wijnen, Epigenetic regulators controlling osteogenic lineage commitment and bone formation, Bone 181 (2024) 117043.

[27] A. Qu, Q. Chen, M. Sun, L. Xu, C. Hao, C. Xu, H. Kuang, Sensitive and selective dual-mode responses to reactive oxygen species by chiral manganese dioxide nanoparticles for antiaging skin, Adv. Mater. 36 (5) (2024) e2308469.

[28] Q. Li, R. Wang, Z. Zhang, H. Wang, X. Lu, J. Zhang, A.P. Kong, X.Y. Tian, H. F. Chan, A.C. Chung, J.C. Cheng, Q. Jiang, W.Y. Lee, Sirt3 mediates the benefits of exercise on bone in aged mice, Cell Death Differ. 30 (1) (2023) 152–167.

[29] Y. Guo, X. Jia, Y. Cui, Y. Song, S. Wang, Y. Geng, R. Li, W. Gao, D. Fu, Sirt3-mediated mitophagy regulates AGEs-induced BMSCs senescence and senile osteoporosis, Redox Biol. 41 (2021) 101915.

[30] J. Zhang, H. Wang, L. Slotabec, F. Cheng, Y. Tan, J. Li, Alterations of SIRT1/SIRT3 subcellular distribution in aging undermine cardiometabolic homeostasis during ischemia and reperfusion, Aging Cell 22 (9) (2023) e13930.

[31] M. Wu, H. Liu, D. Li, Y. Zhu, P. Wu, Z. Chen, F. Chen, Y. Chen, Z. Deng, L. Cai, Smart-responsive multifunctional therapeutic system for improved regenerative microenvironment and accelerated bone regeneration via mild photothermal therapy, Adv. Sci. (Weinh.) 11 (2) (2024) e2304641.

[32] M. Wu, H. Liu, Y. Zhu, F. Chen, Z. Chen, L. Guo, P. Wu, G. Li, C. Zhang, R. Wei, L. Cai, Mild photothermal-stimulation based on injectable and photocurable hydrogels orchestrates immunomodulation and osteogenesis for high-performance bone regeneration, Small 19 (28) (2023) e2300111.

[33] S. Song, G. Zhang, X. Chen, J. Zheng, X. Liu, Y. Wang, Z. Chen, Y. Wang, Y. Song, Q. Zhou, HIF-1α increases the osteogenic capacity of ADSCs by coupling angiogenesis and osteogenesis via the HIF-1α/VEGF/AKT/mTOR signaling pathway, J. Nanobiotechnol. 21 (1) (2023) 257.

[34] Y. Zhang, Z. Hao, P. Wang, Y. Xia, J. Wu, D. Xia, S. Fang, S. Xu, Exosomes from human umbilical cord mesenchymal stem cells enhance fracture healing through HIF-1α-mediated promotion of angiogenesis in a rat model of stabilized fracture, Cell Prolif. 52 (2) (2019) e12570.

[35] K. Hu, B.R. Olsen, Osteoblast-derived VEGF regulates osteoblast differentiation and bone formation during bone repair, J. Clin. Investig. 126 (2) (2016) 509–526.

[36] S. Stegen, N. van Gastel, G. Eelen, B. Ghesquière, F. D'Anna, B. Thienpont, J. Goveia, S. Torrekens, R. Van Looveren, F.P. Luyten, P.H. Maxwell, B. Wielockx, D. Lambrechts, S.M. Fendt, P. Carmeliet, G. Carmeliet, HIF-1α promotes glutamine-mediated redox homeostasis and glycogen-dependent bioenergetics to support postimplantation bone cell survival, Cell Metab. 23 (2) (2016) 265–279.

[37] H. Semba, N. Takeda, T. Isagawa, Y. Sugiura, K. Honda, M. Wake, H. Miyazawa, Y. Yamaguchi, M. Miura, D.M. Jenkins, H. Choi, J.W. Kim, M. Asagiri, A. S. Cowburn, H. Abe, K. Soma, K. Koyama, M. Katoh, K. Sayama, N. Goda, R. S. Johnson, I. Manabe, R. Nagai, I. Komuro, HIF-1α-PDK1 axis-induced active glycolysis plays an essential role in macrophage migratory capacity, Nat. Commun. 7 (2016) 11635.

[38] J.N. Regan, J. Lim, Y. Shi, K.S. Joeng, J.M. Arbeit, R.V. Shohet, F. Long, Up-regulation of glycolytic metabolism is required for HIF1α-driven bone formation, Proc. Natl. Acad. Sci. U. S. A. 111 (23) (2014) 8673–8678.

[39] N. Dirckx, R.J. Tower, E.M. Mercken, R. Vangoitsenhoven, C. Moreau-Triby, T. Breugelmans, E. Nefyodova, R. Cardoen, C. Mathieu, B. Van der Schueren, C. B. Confavreux, T.L. Clemens, C. Maes, Vhl deletion in osteoblasts boosts cellular glycolysis and improves global glucose metabolism, J. Clin. Investig. 128 (3) (2018) 1087–1105.

[40] Y. Liu, N.G. Azizian, D.K. Sullivan, Y. Li, mTOR inhibition attenuates chemosensitivity through the induction of chemotherapy resistant persisters, Nat. Commun. 13 (1) (2022) 7047.

[41] M.M. Ansari, M. Ghosh, D.S. Lee, Y.O. Son, Senolytic therapeutics: an emerging treatment modality for osteoarthritis, Ageing Res. Rev. 96 (2024) 102275.

[42] L. Ma, H. Shi, Y. Li, W. Gao, J. Guo, J. Zhu, Z. Dong, A. Sun, Y. Zou, J. Ge, Hypertrophic preconditioning attenuates myocardial ischemia/reperfusion injury through the deacetylation of isocitrate dehydrogenase 2, Sci. Bull. (Beijing) 66 (20) (2021) 2099–2114.

[43] O. Mossad, B. Batut, B. Yilmaz, N. Dokalis, C. Mezö, E. Nent, L.S. Nabavi, M. Mayer, F.J.M. Maron, J.M. Buescher, M.G. de Agüero, A. Szalay, T. Lämmermann, A. J. Macpherson, S.C. Ganal-Vonarburg, R. Backofen, D. Erny, M. Prinz, T. Blank, Gut microbiota drives age-related oxidative stress and mitochondrial damage in microglia via the metabolite N(6)-carboxymethyllysine, Nat. Neurosci. 25 (3) (2022) 295–305.

[44] H.S. Li, Y.N. Zhou, L. Li, S.F. Li, D. Long, X.L. Chen, J.B. Zhang, L. Feng, Y.P. Li, HIF-1α protects against oxidative stress by directly targeting mitochondria, Redox Biol. 25 (2019) 101109.

[45] H. Xu, B. Ahn, H. Van Remmen, Impact of aging and oxidative stress on specific components of excitation contraction coupling in regulating force generation, Sci. Adv. 8 (43) (2022) eadd7377.
[46] Z. Yang, W. Su, X. Wei, S. Qu, D. Zhao, J. Zhou, Y. Wang, Q. Guan, C. Qin, J. Xiang, K. Zen, B. Yao, HIF-1α drives resistance to ferroptosis in solid tumors by promoting lactate production and activating SLC1A1, Cell Rep. 42 (8) (2023) 112945.
[47] X. Zhou, Y. Qian, L. Chen, T. Li, X. Sun, X. Ma, J. Wang, C. He, Flowerbed-Inspired biomimetic scaffold with rapid internal tissue infiltration and vascularization capacity for bone repair, ACS Nano 17 (5) (2023) 5140–5156.
[48] T. van Vliet, M. Varela-Eirin, B. Wang, M. Borghesan, S.M. Brandenburg, R. Franzin, K. Evangelou, M. Seelen, V. Gorgoulis, M. Demaria, Physiological hypoxia restrains the senescence-associated secretory phenotype via AMPK-mediated mTOR suppression, Mol. Cell 81 (9) (2021) 2041–2052.e6.
[49] J. Moral-Sanz, S.A. Lewis, S. MacMillan, M. Meloni, H. McClafferty, B. Viollet, M. Foretz, J. Del-Pozo, A. Mark Evans, AMPK deficiency in smooth muscles causes persistent pulmonary hypertension of the new-born and premature death, Nat. Commun. 13 (1) (2022) 5034.
[50] G.R. Steinberg, D.G. Hardie, New insights into activation and function of the AMPK, Nat. Rev. Mol. Cell Biol. 24 (4) (2023) 255–272.
[51] W. Cai, S. Mao, Y. Wang, B. Gao, J. Zhao, Y. Li, Y. Chen, D. Zhang, J. Yang, G. Yang, An engineered hierarchical hydrogel with immune responsiveness and targeted mitochondrial transfer to augmented bone regeneration, Adv. Sci. (Weinh.) 11 (42) (2024) e2406287.
[52] J.Y. Wu, P. Aarnisalo, M. Bastepe, P. Sinha, K. Fulzele, M.K. Selig, M. Chen, I. J. Poulton, L.E. Purton, N.A. Sims, L.S. Weinstein, H.M. Kronenberg, Gsα enhances commitment of mesenchymal progenitors to the osteoblast lineage but restrains osteoblast differentiation in mice, J. Clin. Investig. 121 (9) (2011) 3492–3504.
[53] S. Watanuki, H. Kobayashi, Y. Sugiura, M. Yamamoto, D. Karigane, K. Shiroshita, Y. Sorimachi, T. Morikawa, S. Fujita, K. Shide, M. Haraguchi, S. Tamaki, T. Mikawa, H. Kondoh, H. Nakano, K. Sumiyama, G. Nagamatsu, N. Goda, S. Okamoto, A. Nakamura-Ishizu, K. Shimoda, M. Suematsu, T. Suda, K. Takubo, SDHAF1 confers metabolic resilience to aging hematopoietic stem cells by promoting mitochondrial ATP production, Cell Stem Cell (2024) 1145–1161.
[54] B. Wang, D. Vashishth, Advanced glycation and glycoxidation end products in bone, Bone 176 (2023) 116880.
[55] Z. Wang, Y. Zhao, A. Phipps-Green, R. Liu-Bryan, A. Ceponis, D.L. Boyle, J. Wang, T.R. Merriman, W. Wang, R. Terkeltaub, Differential DNA methylation of networked signaling, transcriptional, innate and adaptive immunity, and osteoclastogenesis genes and pathways in gout, Arthritis Rheumatol. 72 (5) (2020) 802–814.
[56] S. Zhang, H. Yang, M. Wang, D. Mantovani, K. Yang, F. Witte, L. Tan, B. Yue, X. Qu, Immunomodulatory biomaterials against bacterial infections: progress, challenges, and future perspectives, Innovation 4 (6) (2023) 100503.
[57] H. Zhou, Z. He, Y. Cao, L. Chu, B. Liang, K. Yu, Z. Deng, An injectable magnesium-loaded hydrogel releases hydrogen to promote osteoporotic bone repair via ROS scavenging and immunomodulation, Theranostics 14 (9) (2024) 3739–3759.
[58] S. Liu, W. Wang, P. Wu, Z. Chen, W. Pu, L. Li, G. Li, J. Zhang, J. Song, Pathogenesis-guided engineering of multi-bioactive hydrogel Co-delivering inflammation-resolving nanotherapy and pro-osteogenic protein for bone regeneration, Adv. Funct. Mater. 33 (32) (2023) 2301523.
[59] D. Wang, Y. Guo, B.C. Heng, X. Zhang, Y. Wei, Y. He, M. Xu, B. Xia, X. Deng, Cell membrane vesicles derived from hBMSCs and hUVECs enhance bone regeneration, Bone Res. 12 (1) (2024) 23.
[60] X. Zhang, C. Chen, C. Ling, S. Luo, Z. Xiong, X. Liu, C. Liao, P. Xie, Y. Liu, L. Zhang, Z. Chen, Z. Liu, J. Tang, EGFR tyrosine kinase activity and Rab GTPases coordinate EGFR trafficking to regulate macrophage activation in sepsis, Cell Death Dis. 13 (11) (2022) 934.
[61] J. Reeves, P. Tournier, P. Becquart, R. Carton, Y. Tang, A. Vigilante, D. Fang, S. J. Habib, Rejuvenating aged osteoprogenitors for bone repair, Elife 13 (2024).
[62] Y. Zhu, H. Liu, P. Wu, Y. Chen, Z. Deng, L. Cai, M. Wu, Multifunctional injectable hydrogel system as a mild photothermal-assisted therapeutic platform for programmed regulation of inflammation and osteo-microenvironment for enhanced healing of diabetic bone defects in situ, Theranostics 14 (18) (2024) 7140–7198.
[63] M. Wu, H. Liu, Y. Zhu, P. Wu, Y. Chen, Z. Deng, X. Zhu, L. Cai, Bioinspired soft-hard combined system with mild photothermal therapeutic activity promotes diabetic bone defect healing via synergetic effects of immune activation and angiogenesis, Theranostics 14 (10) (2024) 4014–4057.
[64] R. Ren, A. Ocampo, G.H. Liu, J.C. Izpisua Belmonte, Regulation of stem cell aging by metabolism and epigenetics, Cell Metab. 26 (3) (2017) 460–474.
[65] F. Liu, L. Yuan, L. Li, J. Yang, J. Liu, Y. Chen, J. Zhang, Y. Lu, Y. Yuan, J. Cheng, S-sulfhydration of SIRT3 combats BMSC senescence and ameliorates osteoporosis via stabilizing heterochromatic and mitochondrial homeostasis, Pharmacol. Res. 192 (2023) 106788.
[66] T. Shimazu, M.D. Hirschey, L. Hua, K.E. Dittenhafer-Reed, B. Schwer, D. B. Lombard, Y. Li, J. Bunkenborg, F.W. Alt, J.M. Denu, M.P. Jacobson, E. Verdin, SIRT3 deacetylates mitochondrial 3-hydroxy-3-methylglutaryl CoA synthase 2 and regulates ketone body production, Cell Metab. 12 (6) (2010) 654–661.
[67] H. Kim, Y.D. Lee, H.J. Kim, Z.H. Lee, H.H. Kim, SOD2 and Sirt3 control osteoclastogenesis by regulating mitochondrial ROS, J. Bone Miner. Res. 32 (2) (2017) 397–406.